# Nonlinear waveform steepening in time reversal focusing of airborne, one-dimensional sound waves, and the absence of Mach stems

Michael M. Hogg

A senior thesis submitted to the faculty of

Brigham Young University

in partial fulfillment of the requirements for the degree of

Bachelor of Science

Brian E. Anderson, Advisor

Department of Physics and Astronomy

Brigham Young University

August 2025

Copyright © 2025 Michael M. Hogg

All Rights Reserved

# ABSTRACT

Nonlinear waveform steepening in time reversal focusing of airborne, one-dimensional sound waves, and the absence of Mach stems

Michael M. Hogg

Department of Physics and Astronomy, BYU

Bachelor of Science

Time reversal (TR) is a process that can be used to generate high amplitude focusing of sound. It has been previously shown that high amplitude focused sound using TR in reverberant environments exhibits multiple nonlinear features including waveform steepening and a nonlinear increase in peak compression pressures. This study investigates the removal of one possible cause for these phenomena: free-space Mach stems. By constraining the focusing in the system to one dimensional (1-D) waves, the potential formation of Mach stems is eliminated so that remaining effects can be observed. A system of pipes is used to restrict the focused waves to be planar in a 1-D reverberant environment. Results show that waveform steepening effects remain as expected but that the nonlinear increase in compression amplitudes disappears because Mach stems cannot form in a 1-D system. These experiments provide evidence in favor of the assertion that free-space Mach stems cause the nonlinear increase in compression pressures when creating TR focusing in multiple dimensions.

Keywords: Time Reversal, Finite Amplitude, Nonlinear Acoustics, Waveguides

ACKNOWLEDGMENTS

I would like to thank Brian Anderson and Brian Patchett for introducing me into the world of nonlinear acoustics and for teaching me practically everything I know about this field. I would further like to thank Jay Cliftmann, Andrew Basham, and Adam Kingsley for much help with ideas for measurements, programming and initial concepts for physical phenomena in my many datasets. I also would like to acknowledge the BYU College of Computational, Mathematical, and Physical Sciences for providing funding for my research throughout my time here. Finally, I would like to give a huge thanks to my family for putting up with my increasingly jargon filled paragraphs every time I would talk about what I was doing in research.

.

# Table of Contents



.

# List of Figures

# Chapter 1

# Introduction

Time Reversal (TR) is a signal processing technique that can be used to focus physical waves, acoustic or otherwise, to a selected spatial location in a system.[1-4] Historically, acoustic TR was first used as a method to create localized and reproduceable underwater communications[5-6] that were difficult to intercept. More recent studies in communications have shown that TR allows for long distance communication in an ocean environment[7-8] and communication in among a network of pipes.[9] Other uses for TR involve source localization in which waves propagate back through the environment to their original emission location.[10-12] There is also high amplitude focusing of sound and vibration, which is the main use of TR that the present study is concerned with.[4] Studies of high amplitude focusing have investigated localized delivery of energy for many purposes, including non-destructive evaluation to find cracks[3,13-14] or evaluate a structure's response to sound,[15-17] nonsurgical biomedical treatment,[18-20] and focusing sound loud enough to study nonlinear features in that focused sound.[21-23]

TR focusing relies on obtaining the impulse response from a source to a receiver. In a reverberant environment the energy emitted from an impulsive emission takes many paths to the receiver. The arrival times of the reflections about the room are thus encoded in the impulse response. If this impulse response is time reversed and broadcast from the source, the paths that were initially traversed, when the impulse response was obtained, are retraced such that energy simultaneously arrives at the receiver location from all these paths. These simultaneous arrivals

constructively interfere resulting in high amplitude focusing of sound at the receiver location. In a reverberant environment, arrivals can come from all directions resulting in an approximately converging spherical wave[24] made up of many diverging spherical waves (an expression of Huygen's principle). Multiple sources may be used in TR and when their reversed impulse responses are synchronously timed the amplitude of the focus is further increased.

As waves are being focused using TR, they are relatively low in amplitude before they converge at the focal location. However, at the focal location, whose spatial extent is roughly one wavelength in diameter, the peak amplitude can be three times higher on average than the amplitude of the converging waves. Thus, nonlinear features are more likely to be observed at the focal location than in the converging waves prior to focusing. This phenomenon is exploited when TR is used for nondestructive evaluation applications since the focusing is localized, and when the focusing occurs at a location on a sample that vibrates nonlinearly (i.e. a crack or delamination), then more nonlinearity may be observed in focusing at that location than when focusing at other intact locations on a sample.[14,25-28] Wallace and Anderson[29] showed that localized high amplitude focusing of two ultrasound frequencies in air could create an audible difference frequency. In biomedical ultrasound applications, waves focused with TR can generate localized heating at the focal location and be used to destroy kidney stones and brain tumors.[18-20] There are other ways to create High Intensity Focused Ultrasound (HIFU) for biomedical applications besides using TR. In HIFU experiments and modeling, an increase in compression amplitudes and a decrease in rarefaction amplitudes has been observed[30] but the physical mechanism was not explained.

Two nonlinear features have been asserted to happen during high amplitude TR focusing, waveform steepening and Mach stem formation.[22-23] In nonlinear acoustics, waveform steepening is due to an increase in wave speed in the compressions of the wave, and a decrease of speed in

the rarefactions of the wave as it propagates; both of which are breakdowns of the linear acoustics assumptions.[31] Thus, sine waves evolve into sawtooth waveforms with shocks present where the slope of the waveform is infinite.[32] When wave steepening occurs, the peak compression amplitudes are reduced relative to linear scaling as the wave continues to propagate. This feature causes a shifting of energy from the fundamental frequency to higher harmonics as the waveform steepens. Mach stems form when high pressure wave fronts interfere and interact with one another.[23,33-36] One finite amplitude wave leaves behind excess heat in the medium (a breakdown of the adiabatic assumption), thereby increasing the sound speed in the medium behind it, and this increase in speed allows a trailing wave to catch up to the leading wave. This means Mach stems are typically observed in two-dimensional and three-dimensional environments where these types of interactions can occur. Unlike wave steepening, the compression amplitude in a Mach stem nonlinearly increases, producing pressures that are larger than the linear sum of the two constituent waves.

Montaldo *et al*.[37] reported data that exhibited nonlinear behavior in high amplitude TR focusing of ultrasound in a lithotripsy application. In their setup, as pulse excitation voltage was increased the resulting focal signal exhibited increasing levels of nonlinearity, particularly waveform steepening, but not nonlinear amplification. Willardson *et al.*[21] reported nonlinearities in high amplitude TR focusing of audible frequency sound in a reverberation chamber, with a nonlinear increase of peak pressure in higher input amplitudes. They contrasted their results with those of Montaldo *et al.* and pointed out that the results reported by Montaldo *et al.* show a nonlinear decrease of compressions; nonlinearity wasn't discussed by Montaldo *et al.* Patchett and Anderson[22] furthered the work of Willardson *et al.* and created a peak focal pressure in air of 214.8 kPa or 200.6 $dB_{peak}$. This amplitude was approximately two times higher than linear scaling would

have predicted.[22] Willardson *et al.*[21] and Patchett and Anderson[22] cite wave steepening as a possible contributing factor in their results. Patchett and Anderson further claim that free-space Mach stem formation is the mechanism of the nonlinear increase shown in the high amplitude compressions. This later claim was more fully studied by Patchett *et al*.,[23] where they used numerical modeling to show that free-space Mach stem formation occurs in high amplitude TR when the high-pressure waves are allowed to interact. They also showed that when the TR focusing comes from a limited aperture (i.e. from a limited range of angles of incidence) that the nonlinear increase from Mach stems doesn't happen. This explains why it didn't happen in the results reported by Montaldo *et al.* where waves in their setup converged from a limited aperture but they were not constrained to propagate as plane waves in a waveguide. What is currently unknown is if a nonlinear increase would be observed in a system where wavefronts cannot overlap, meaning a case where Mach stems cannot form.

The purpose of this thesis is to experimentally show that in a system in which waves are constrained to travel in one dimension, where Mach stems cannot form, that nonlinear amplification of peak compressions no longer happens. Thus, the observed nonlinearity that remains appears to be limited solely to waveform steepening. TR focusing experiments conducted in a room with waves converging in three dimensions are compared to TR focusing experiments conducted in a network of pipes with sound waves restricted to converge in one dimension. The bandwidth used for both sets of experiments, of 500 – 3500 Hz, restricts wave propagation to plane waves within the pipes. Experiments in both acoustic systems are conducted at sound levels where finite-amplitude, nonlinear effects are observed.

# Chapter 2

# Experimental Setup

The measurements for this study took place within a system of pipes. The pipes are made of cast iron, which should ensure very little excitation of pipe wall vibration due to the acoustic pressure waves. Waves inside the pipes reflect off of hard wall boundaries and the only losses come from propagation (e.g. molecular relaxation) and thermoviscous boundary losses. Thus, the internal environment is considered reverberant albeit with a reverberation time of $75 \pm 4.5$ ms. The pipes have a 5.08 cm (2 inch) inner diameter which were connected by various pieces that accommodate junctions of 2, 3, or 4 pipes in total. These junction pieces are referred to as couplers, T-pieces, and cross-pieces. In conjunction with various lengths of pipe, eight BMS (Hannover, Germany) 4590 dual-diaphragm, high-output loudspeakers are fitted with appropriate crossover circuits and bolted to the ends of the pipes with flanges. Figure 2.1 shows a photograph of the actual system of pipes and loudspeakers used for the experiment. Notice that the length of the branches of the system are varied to prevent the formation of degenerate modes and to spread out the timing of reflections arrivals at the microphone. An important feature is the straight section in the middle which is meant to let the plane waves propagate a distance in only a single duct before arriving at the microphone, a GRAS (Holte, Denmark) 46BG at the center of this linear section, kept in the center of the pipe via some foam. At the ends of each of the branches are the loudspeakers previously mentioned.

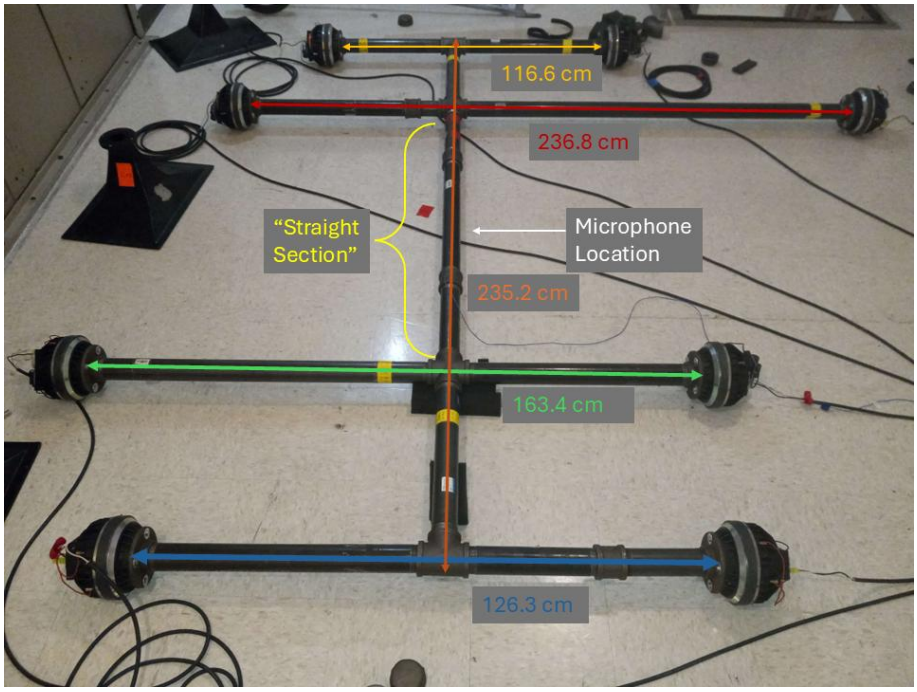


FIG. 2.1. Photograph of the system of pipes used to create the one-dimensional environment. Main lengths (measured from outer flange end to outer flange end) and locations are labeled.

The TR process was carried out via a custom LABVIEW™ (Austin, TX) executable program developed in-house,[38] coupled with two Spectrum Instrumentation (Großhansdorf, Germany) M2i.6022 signal generation cards and a M2i.4931 digitizer card. The signals from the cards are output to two Crown (Elkhart, IN) CT4150 amplifiers which send the signal to the loudspeakers. Typical TR processing is used in this study since we can see the nonlinearities without using the clipping TR method used by Patchett and Anderson.[22] This decision was informed by the observations of odd amplitude related effects in preliminary data at extreme sound levels, and these effects were decided to be out of the scope of the thesis.

To guarantee one-dimensional propagation of waves in the system, the bandwidth of frequencies used in these experiments was limited to those below the plane wave tube cutoff frequency. The plane wave cutoff frequency for a circular duct is given by,

$$f_c = \frac{1.841c}{2\pi a}, \tag{2.1}$$

where $c$ is the speed of sound and $a$ is the radius of the duct. For our system, we decided to limit our bandwidth to below 3500 Hz, which is well below $f_c$ (approximately 3950 Hz) and used that as our maximum input frequency. A swept sine wave signal, or chirp signal, was created as the input signal to the system. A bandwidth of 500 – 3500 Hz was used to generate the chirp signal, with the lower frequency being determined by the limitation of the drivers themselves. Note that Golightly *et al.*[39] also conducted TR experiments with plane waves in pipes but restricted their study to much lower sound levels for the purpose of exploring a super resolution concept.

The specific TR process we use for these measurements is reciprocal TR,[2] which consists of a forward step and a backward step. During the forward step a chirp signal is broadcast into the system from each driver, individually in turn. The microphone records the response of the system from each of the sources; these data are known as the chirp response (CR). A cross-correlation is performed between the chirp signal and the CR resulting in an impulse response (IR) of the system. This IR is then reversed in time to produce the time reversed impulse response (TRIR). During the backward step the TRIR signals are simultaneously broadcast from all sources into the system. The direct propagation delay from the source and timing of reflections that arrive at the microphone are encoded into the TRIR and upon broadcast of the TRIR, energy will partially retrace these paths and thus a convergence of waves will constructively interfere at the location of the microphone. The resulting superposition of the focusing produced by each of the 8 sources broadcasting their TRIR signals is recorded at the focus position by the microphone. This focusing of sound is repeated with different levels of amplification and these focal signals are linearly scaled and compared to look for differences as the input amplitudes are increased.

With that process in mind, the following settings were used. The chirp signal had a length of 4.16 s with 0.34 s of trailing zeroes to allow ample time for the reverberation to dampen in preparation for the broadcast of the chirp signal from the next driver. The frequency progression in the chirp was logarithmic to match that of Patchett and Anderson[22] and had a bandwidth of 500 – 3500 Hz due to the limitations mentioned previously. A sampling frequency of 250 kHz is used both for the generation of the signals and their recording. The chirp signals are output from the sound card with a peak amplitude of 100 mV into the amplifier. The amplitude of signals output from the sound cards and input to the amplifier will thusly be called an input amplitude. After the CRs are recorded and processed into the eight individual TRIRs, we are ready to take the measurements needed. The sound cards can generate output amplitudes of 100 mV to 1800 mV and it was determined to use 3 dB increases for the input amplitude levels (multiplying the previous input level by $\sqrt{2}$) beginning at 100 mV and stopping at 1600 mV. This produces nine increasing levels of output from the audio cards (100 mV, 141 mV, 200 mV, 282 mV, 400 mV, 565 mV, 800 mV, 1131 mV, and 1600 mV).

For comparison to the pipe system, a standard TR experiment was done inside the small reverberation chamber at Brigham Young University. This reverberation chamber has dimensions 5.7 m × 4.3 m × 2.5 m. The overall reverberation time in the room is approximately 3.16 ± 0.08s across the chirp bandwidth used, and the room has a Schroeder frequency of 522 Hz. The physical setup matches the setup of Patchett and Anderson.[22] This includes the drivers being mounted to horns and facing away from the microphone,[40] which was placed in a corner of the room.[41] The same bandwidth of 500 – 3500 Hz and input amplitudes are used in the room experiments as in the pipe experiments except for the trailing zeroes length being longer at 3.84 seconds to account for the longer reverberation time in the room.

# Chapter 3

# Results

To allow a linear scaling analysis, each TR focus time signal was multiplied by a scaling factor, $S$,

$$S = \frac{1600}{I}, \tag{3.1}$$

where $I$ is the input amplitude in mV generated from the sound cards. For linear cases this would generate copies of the highest amplitude signal. If nonlinearities are present, the scaling factor allows identification of differences between the results of using lower amplitude inputs and higher amplitude inputs to the system. Figure 3.1(b) shows example results from three superimposed TR focus time signals recorded when performing TR in the 1D pipe system, with each input amplitude spaced by 12 dB. We observe that as the input amplitude increases the scaled peak compression amplitude decreases. This indicates a nonlinear suppression of compressions as the amplitude from the drivers increases. Notably this finding is contrary to the findings of Willardson *et al.*[21] and Patchett and Anderson,[22] whose experiments were done with three-dimensional wave focusing in a room, but was expected here since this experiment is done solely with one dimensional waves, where Mach stems are not expected to form. Additionally, the higher amplitude focus peak arrives earlier in time with a steepening of the leading edge of the wave, indicating waveform steepening. This coincides with the claims of Willardson *et al.*,[21] Patchett and Anderson,[22] and Patchett *et al.*[23] who all asserted that waveform steepening is present in higher

amplitude focus signals. The results shown in Fig. 3.1(b) are exemplary of many experiments done at various amplitudes within the pipes under various conditions.

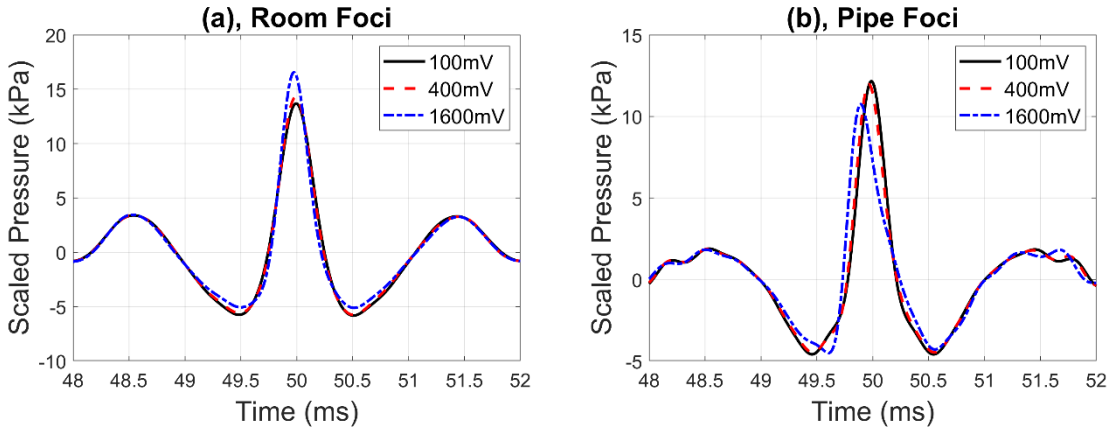


FIG. 3.1. (a) Scaled time reversal focus signals when focusing 3D sound within a room. Note the increase of scaled peak compression amplitude and earlier arrivals of the peak compression. (b) Scaled time reversal focus signals when focusing 1D sound within pipes. Note the decrease of scaled peak compression amplitudes and earlier arrivals of the peak compression.

These TR focusing results in the pipes are now contrasted with TR focusing results obtained in a room using similar settings (the microphone was placed in a corner of the room as was done by Patchett and Anderson[22]). Figure 3.1(a) shows TR focus signals when using the same input amplitudes in a room as used in the pipes. Similar features as those reported by Patchett and Anderson[22] are observed; namely, as the amplitude from the drivers increases, a nonlinear increase in the peak compression amplitude is observed (nonlinear amplification) along with a nonlinear suppression of the rarefactions on either side of that main focal peak. Steepening of the waveform is also observed. The key difference between these two sets of results is the 1D environment for the pipes and the 3D environment for the room. The nonlinear amplification of peak compression and nonlinear suppression of the adjacent

rarefactions was also reported by Willardson *et al.*[21] and by Patchett and Anderson[22] though here a narrower bandwidth of frequencies was used. Willardson *et al.*[21] and Patchett and Anderson[22] claimed these features were the result of Mach stem formation with the overlapping of high-pressure waves. Patchett *et al.*[23] showed through numerical modeling that indeed Mach stem formation in collapsing waves allows additional energy to arrive at the time of maximal focusing causing the nonlinear amplification of compressions.

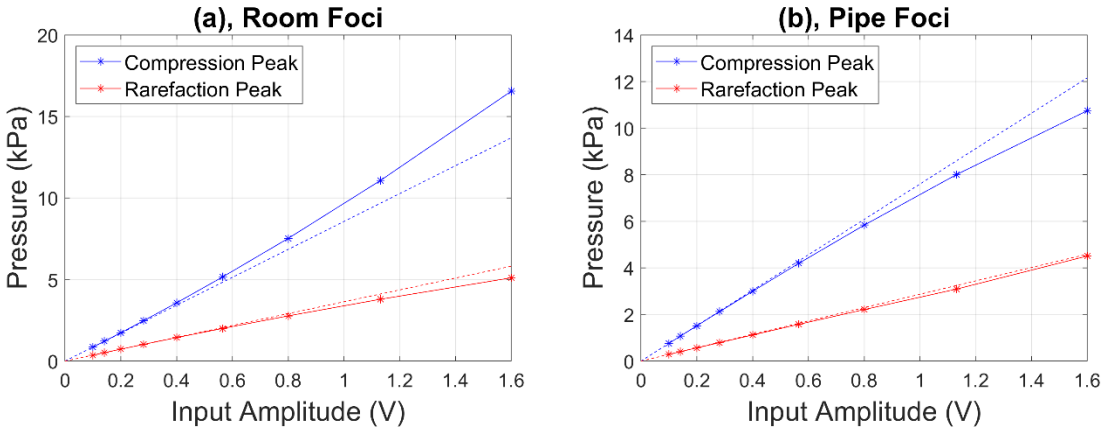


FIG. 3.2 Peak amplitudes of the primary compression of the time reversal focus and the peak amplitudes of the largest rarefaction shown at each of 9 input amplitudes as compared with the linear case (extrapolating linearly from the lowest amplitude). (a) 3D focusing of sound in a room (b) 1D focusing of sound in pipes.

We show further that as the input amplitude increases, we depart further from linearity. Figure 3.2 shows the peak amplitudes of the main focal compressions and the peak amplitudes of the largest rarefactions for various input amplitudes as compared to linear scaling of the peak compression and rarefaction pressures that the 100 mV input creates. It is clear that there is a nonlinear suppression of the higher amplitudes for both the compressions and rarefactions. The nonlinear suppression of the rarefaction amplitude is consistent with what is found by Patchett and Anderson[22] but the compression amplitude progression shows the opposite here; a decrease

relative to linear scaling is observed in pipes rather than a nonlinear increase in peak compression pressures in rooms as input amplitude increases. Compare Fig. 3.2 here to Fig. 8 by Patchett and Anderson.[22]

Figure 3.3(a) shows example focal signals for the minimum and maximum input voltages. Additional lines have been drawn on this figure to aid in quantifying metrics related to nonlinearity exhibited in the focal signals as a function of input voltage. The difference in the scaled, peak compression amplitudes is apparent in this figure. The variation of these peak amplitudes is shown as a function of input voltage in Fig. 3.3(b). As noted previously, the peak amplitudes nonlinearly increase in the room and nonlinearly suppress in the pipes with increasing input voltage. Along with the nonlinear suppression, we observe an increase in the wave steepening of the leading edge of the main compression peak as quantified by the maximum slope/derivative, which is to say that steepening increases with increasing input amplitude. Consistent with wave steepening effects, the peak compressions arrive progressively earlier with increasing input amplitude. In Fig. 3.3(a) the arrival times are denoted by vertical lines and the variation as a function of input amplitude is shown in Fig. 3.3(c). Note that the variation in the arrival times is more dramatic in the pipes than in the room. The earlier arrival of the peaks in the room results is consistent with Patchett and Anderson's findings.[22] This effect is more pronounced in the pipes as nonlinearities are more easily generated in one-dimensional propagation (focusing of waves in a pipe) than in three-dimensional propagation (focusing of waves in a room). In Fig. 3.3(a), the maximum derivative of each signal is denoted by a circle with a tangent line drawn. In Fig. 3.3(d), the variation of maximum derivative is shown as a function of input amplitude, with a minor difference between the data in the pipes and in the room at the highest amplitudes. If everything scaled linearly in these two experiments, then no nonlinear amplification or suppression of the main compression peaks would be observed.

The arrival times of the peak compressions would not change and the derivatives of the leading edge of the compression would not change either.

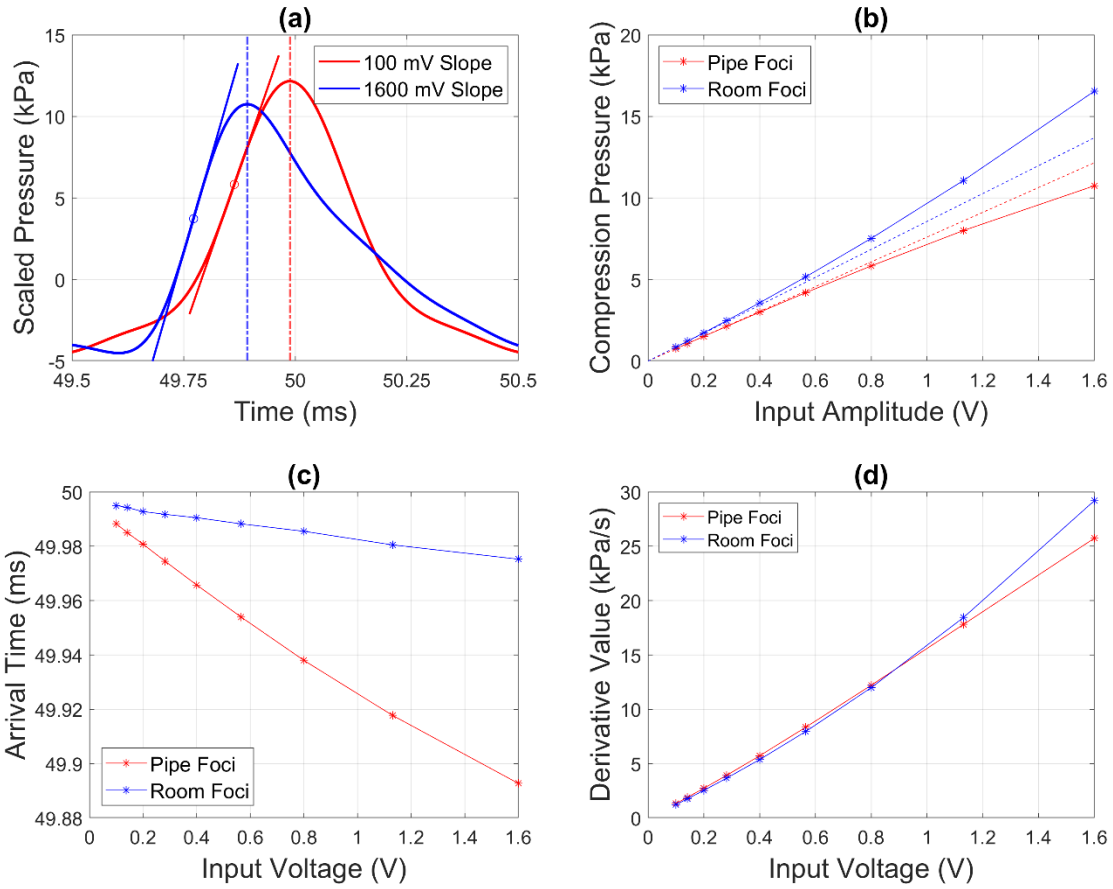


FIG. 3.3 (a) A low and high amplitude focal signal are compared. Maximum derivative of the leading edge of the main compression peak in each focal signal are denoted by circles with tangent lines that possess the respective maximum slopes. The vertical, dash-dotted lines denote the time of maximum compression amplitude for each focal signal. (b) Peak compression amplitudes of time reversal focusing in pipes and in the room, which data is shown in Fig. 3.2. (c) Arrival times for the peak compression amplitudes in pipes and in the room. (d) Maximum derivative values from the data in pipes and in the room.

# Chapter 4

# Conclusion

In this environment where only one-dimensional plane waves may propagate, high amplitude Time Reversal (TR) focusing yields a nonlinear suppression or decrease of the peak compression amplitude as the input amplitude is increased. In addition, it was found that the peak compression of the focusing arrives earlier in time and has a higher valued slope/derivative of the leading edge of the main focal compression. These effects are consistent with the ideas of waveform steepening and shock wave formation. Thus, by restricting the wave propagation to one-dimensional planes waves in the pipe system, the potential for Mach stem formations is eliminated and no nonlinear amplification of the compression amplitude is observed. This experimental finding is consistent with the Mach stem explanation for the nonlinear amplification reported by Willardson *et al.*[21] and Patchett and Anderson[22] and explored through numerical simulations by Patchett *et al.*[23]

# References


[1] M. Fink, "Time Reversed Acoustics," Phys. Today **50**, 34–40 (1997).

[2] B. E. Anderson, M. Griffa, P. A. Johnson, C. Larmat, and T. J. Ulrich, "Time reversal," Acoust. Today **4**(1), 5-16 (2008).

[3] B. E. Anderson, M. C. Remillieux, P.-Y. Le Bas, and T. J. Ulrich, "Time reversal techniques," Chapter 14 in *Nonlinear Acoustic Techniques for Nondestructive Evaluation, 1st Edition*, Editor Tribikram Kundu, ISBN: 978-3-319-94476-0 (Springer and Acoustical Society of America), pp. 547-581 (2019).

[4] B. E. Anderson, "High amplitude time reversal focusing of sound and vibration," Proc. Meet. Acoust. **51**, 032001 (2023).

[5] A. Parvulescu and C. Clay, "Reproducibility of signal transmissions in the ocean," Radio and Electron. Eng. **29**(4), 223–228 (1965).

[6] C. S. Clay and B. Anderson, "Matched signals: The beginnings of time reversal," Proc. Meet. Acoust. **12**, 055001 (2011).

[7] H. C. Song, "An overview of underwater time-reversal communication," IEEE J. Ocean Eng. **41**(3), 644-655 (2016).

[8] H. C. Song, G. Byun, and J. S. Kim, "Remote acoustic illumination using time reversal and a surface ship," J. Acoust. Soc. Am. **145**(3), 1565-1568 (2019).

[9] B. E. Anderson, T. J. Ulrich, P.-Y. Le Bas, and J. A. Ten Cate, "Three-dimensional time reversal communications in elastic media," J. Acoust. Soc. Am. **139**(2), EL25–EL30 (2016).

[10] C. S. Larmat, R. A. Guyer, P. A. Johnson, "Time-reversal methods in geophysics," *Phys. Today* **63**(8)*,* 31-35 (2010).

[11] S. Cheinet, L. Ehrhardt, T. Broglin, "Impulse source localization in an urban environment: Time reversal versus time matching," *J. Acoust. Soc. Am.* **139**(1), 128-140 (2016).

[12] A. Mimani, Z. Prime, D. J. Moreau, C. J. Doolan, "An experimental application of aeroacoustic time-reversal to the Aeolian tone," *J. Acoust. Soc. Am.* **139**(2), 740-763 (2016).

[13] B. E. Anderson, M. Griffa, T. J. Ulrich, P.-Y. Le Bas, R. A. Guyer, and P. A. Johnson, "Crack localization and characterization in solid media using time reversal techniques," *in Proceedings of the 44th U.S. Rock Mechanics Symposium and 5th U.S.-Canada Rock Mechanics Symposium*, paper No. ARMA-10-154 (2010).

[14] S. M. Young, B. E. Anderson, S. M. Hogg, P.-Y. Le Bas, and M. C. Remillieux, "Nonlinearity from stress corrosion cracking as a function of chloride exposure time using the time reversed elastic nonlinearity diagnostic," *J. Acoust. Soc. Am.* **145**(1), 382–391 (2019).

[15] P.-Y. Le Bas, M. C. Remillieux, L. Pieczonka, J. A. Ten Cate, B. E. Anderson, and T. J. Ulrich, "Damage imaging in a laminated composite plate using an air-coupled time reversal mirror," Appl. Phys. Lett. **107**, 184102 (2015).

[16] M. Farin, C. Prada, T. Lhommeau, M. El Badaoui, J. de Rosny, "Towards a remote inspection of jet engine blades using time reversal," J. Sound Vib. **525**, 116781 (2022).

[17] R. S. Russell, B. E. Anderson, and M. H. Denison, "Using time reversal with long duration broadband noise signals to achieve high amplitude and a desired spectrum at a target location," Appl. Acoust. **236**, 110744 (2025).

[18] J.-L. Thomas, F. Wu, and M. Fink, "Time reversal focusing applied to lithotripsy," *Ultrason. Imag.* **18**(2), 106–121 (1996).

[19] M. Tanter, J.-L. Thomas, and M. Fink, "Focusing and steering through absorbing and aberrating layers: Application to ultrasonic propagation through the skull," *J. Acoust. Soc. Am.* **103**(5), 2403–2410 (1998).

[20] J.-L. Thomas and M. Fink, "Ultrasonic beam focusing through tissue inhomogeneities with a time reversal mirror: Application to transskull therapy," *IEEE Trans. Ultrason. Ferroelectr. Freq. Control* **43**(6), 1122–1129 (1996).

[21] M. L. Willardson, B. E. Anderson, S. M. Young, M. H. Denison, and B. D. Patchett, "Time reversal focusing of high amplitude sound in a reverberation chamber," J. Acoust. Soc. Am. **143**(2), 696–705 (2018).

[22] B. D. Patchett and B. E. Anderson, "Nonlinear characteristics of high amplitude focusing using time reversal in a reverberation chamber," J. Acoust. Soc. Am. **151**(6), 3603–3614 (2022).

[23] B. D. Patchett, B. E. Anderson, and A. D. Kingsley, "Numerical modeling of Mach-stem formation in high-amplitude time-reversal focusing," J. Acoust. Soc. Am. **153**(5), 2724–2732 (2023).

[24] B. E. Anderson, T. J. Ulrich, and P.-Y. Le Bas, "Comparison and visualization of the focusing wave fields of various time reversal techniques in elastic media," J. Acoust. Soc. Am. **134**(6), EL527-EL533 (2013).

[25] T. J. Ulrich, P. A. Johnson, and A. Sutin, "Imaging nonlinear scatterers applying the time reversal mirror," J. Acoust. Soc. Am. **119**(3), 1514–1518 (2006).

[26] T. J. Ulrich, A. M. Sutin, T. Claytor, P. Papin, P.-Y. Le Bas, and J. A. TenCate, "The time reversed elastic nonlinearity diagnostic applied to evaluation of diffusion bonds," Appl. Phys. Lett. **93**(15), 151914 (2008).

[27] B. E. Anderson, M. Griffa, T. J. Ulrich, P.-Y. Le Bas, R. A. Guyer, and P. A. Johnson, "Crack localization and characterization in solid media using time reversal techniques," Am. Rock Mech. Assoc., #10-154 (2010).

[28] S. Dos Santos and Z. Prevorovsky, "Imaging of human tooth using ultrasound based chirp-coded nonlinear time reversal acoustics," Ultrasonics **51**(6), 667–674 (2011).

[29] C. B. Wallace and B. E. Anderson, "High-amplitude time reversal focusing of airborne ultrasound to generate a focused nonlinear difference frequency," J. Acoust. Soc. Am. **150**(2), 1411-1423 (2021).

[30] M. S. Canney, M. R. Bailey, L. A. Crum, V. A. Khokhlova, and O. A. Sapozhnikov, "Acoustic characterization of high intensity focused ultrasound fields: A combined measurement and modeling approach," J. Acoust. Soc. Am. **124**(4), 2406-2420 (2008).

[31] S. L. Garrett, *Understanding acoustics*, 2nd Ed., (Springer and Acoustical Society of America, New York, 2020), pp. 358-373.

[32] M. F. Hamilton and D. T. Blackstock, *Nonlinear acoustics*, (Academic Press, San Diego, 1998), pp. 1-23, 138.

[33] G. Ben-Dor, *Shock Wave Reflection Phenomena*, (Springer Verlag, New York, 1992), pp. 3–13.

[34] M. M. Karzova and V. A. Khokhlova, "Mach stem formation in reflection and focusing of weak shock acoustic pulses," J. Acoust. Soc. Am. **137**(6), EL436–EL442 (2015).

[35] J. N. Tjotta and S. Tjotta, "Nonlinear equations of acoustics, with application to parametric acoustic arrays," J. Acoust. Soc. Am. **69**(6), 1644–1652 (1981).

[36] E. C. Hansen, A. Frank, P. Hartigan, and K. Yirak, "Numerical simulations of Mach stem formation via intersecting bow shocks," High Energy Density Phys. **17**, 135–139 (2015).

[37] G. Montaldo, P. Roux, A. Derode, C. Negreira, and M. Fink, "Ultrasound shock wave generator with one-bit time reversal in a dispersive medium, application to lithotripsy," Appl. Phys. Lett. **80**, 897–899 (2002).

[38] A. D. Kingsley, J. M. Clift, B. E. Anderson, J. E. Ellsworth, T. J. Ulrich, and P.-Y. Le Bas, "Development of software for performing acoustic time reversal with multiple inputs and outputs," Proc. Meet. Acoust. **46**, 055003 (2022).

[39] E. D. Golightly, B. E. Anderson, A. D. Kingsley, R. Russell, and R. Higgins, "Super resolution, time reversal focusing using path diverting properties of scatterers," Appl. Acoust. **206**, 109308 (2023).

[40] B. E. Anderson, M. Clemens, and M. L. Willardson, "The effect of transducer directionality on time reversal focusing," J. Acoust. Soc. Am. **142**(1), EL95-El101 (2017).

[41] B. D. Patchett, B. E. Anderson, and A. D. Kingsley, "The impact of room location on time reversal focusing amplitudes," J. Acoust. Soc. Am. **150**(2), 1424-1433 (2021).